Environ. Sci. Technol. **1999**, *33,* 4022−4028

Influence of Aqueous and Solid-Phase Fe(II) Complexants on Microbial Reduction of Crystalline Iron(III) Oxides†

MATILDE M. URRUTIA,*,‡
ERIC E. RODEN,‡ AND
JOHN M. ZACHARA§

Department of Biological Sciences, The University of Alabama, Box 870206, Tuscaloosa, Alabama 35487-0206, and Pacific Northwest National Laboratory, P.O. Box 999, Environmental Dynamics & Simulation Department, W. R. Wiley Environmental Molecular Sciences Lab, Mail Stop K8-96, Richland, Washington 99352

The influence of aqueous (NTA and EDTA) and solid-phase (aluminum oxide, layer silicates) Fe(II) complexants on the long-term microbial reduction of synthetic goethite by *Shewanella alga* strain BrY was studied. NTA enhanced goethite reduction by promoting aqueous Fe(II) accumulation, in direct proportion to its concentration in culture medium (0.01−5 mM). In contrast, EDTA failed to stimulate goethite reduction at concentrations ≤1 mM, and 5 mM EDTA enhanced the final extent of reduction by only 25% in relation to nonchelator controls. The minor effect of EDTA compared to NTA, despite the greater stability of the Fe(II)−EDTA complex, likely resulted from sorption of Fe(II)−EDTA complexes to goethite. Equilibrium Fe(II) speciation calculations showed that $Fe(II)_{aq}$ should increase with NTA at the expense of the solid-phase Fe(II) species, whereas the opposite trend was true for EDTA due to Fe(II)EDTA adsorption. The presence of aluminum oxide and layer silicates led to a variable but significant (1.5 to > 3-fold) increase in the extent of goethite reduction. Speciation of Fe(II) verified the binding of Fe(II) by these solid-phase materials. Our results support the hypothesis that iron(III) oxide reduction may be enhanced by aqueous or solid-phase compounds which prevent or delay Fe(II) sorption to oxide and FeRB cell surfaces.

Introduction

Microbial iron(III) oxide reduction strongly influences the geochemistry of anaerobic soil and sedimentary environments as well as the persistence and mobility of various types of organic and inorganic contaminants in such environments (*1, 2*). Recent studies indicate that the surface chemical properties of both the iron(III) oxide and the dissimilatory Fe(III)-reducing bacteria (FeRB) control the initial rate and long-term extent of microbial reduction of synthetic iron(III) oxides in defined growth medium (*3, 4*). Fe(II) coatings on the surface of iron(III) oxides and FeRB lead to deactivation of Fe(III) reduction as oxide and cell surface sites become saturated with sorbed Fe(II). However, reduction can proceed to greater levels than the measured Fe(II) sorption capacity if conditions favor bacterial growth (*3*). The importance of surface saturation as a passivation mechanism is supported by the observations that Fe(III) reduction can be reactivated if sorbed Fe(II) is removed from the oxide surface (*4*) or if fresh FeRB cells are added to Fe(II)-saturated materials (*3*). Our findings suggest that the extent of iron(III) oxide reduction in anaerobic environments may be influenced by reactions with associated solid phases and aqueous ligands that compete for and complex Fe(II) produced during oxide reduction.

Synthetic chelators such as EDTA and NTA have been shown to play an important role in metal/radionuclide speciation, solubility, and mobility in surface waters and groundwater (*5*−*11*). EDTA and NTA complex both Fe(III) and Fe(II) and may therefore influence the microbial reduction of iron(III) oxides by both dissolution (*12*) and Fe(II) sequestration (our untested hypothesis). Biogenic Fe(II) may exert a strong impact on the stability of mobile metal/radionuclide complexes by displacement reactions (*13*).

Fe(II)-sorbing mineral phases, such as aluminum oxides and layered silicates, may function as alternate sinks for Fe(II), thereby decreasing or delaying iron(III) oxide and bacterial surface saturation with Fe(II). Fe(II) binding by these phases could thus have a direct impact on the activity of FeRB in soil and sedimentary environments as well as the geochemical conditions influenced by their activity, including groundwater pH, alkalinity, and biomineralization. These geochemical effects may strongly influence the mobility of contaminant metals and radionuclides in anaerobic subsurface environments.

In this paper we investigate the influence of aqueous (NTA, EDTA) and solid-phase (aluminum oxide and layer silicates) complexants on the rate and extent of bacterial iron(III) oxide reduction. Our central hypothesis was that Fe(II) complexation would enhance the long-term reducibility of iron(III) oxides by delaying the formation of passivating oxide/cell surface Fe(II) coatings. Results indicate that all of these Fe(II) ligands have the potential to enhance microbial reduction of crystalline iron(III) oxides to some extent, but the biogeochemical interactions are complex and effects are nonlinear.

Material and Methods

Organism and Culture Conditions. The dissimilatory Fe(III)- and Mn(IV)-reducing bacterium *Shewanella alga* strain BrY(*14*) was used as a test organism. *S. alga* was grown anaerobically in basal culture medium with H_2 as electron donor, malate (30 or 8 mM as indicated) as carbon source, and synthetic goethite (50 mmol L^{-1}; 4.45 g L^{-1}) as electron acceptor in which the PO_4^{3-} concentration was reduced 100-fold (to 0.04 mM) relative to the original (*15*) basal salts composition. The medium was autoclaved prior to the addition of H_2 gas. *S. alga* was grown aerobically to late exponential phase in Tryptic Soy Broth (TSB). The TSB-grown cells were washed once with 10 mM Pipes buffer (piperazine-*N*,*N*′-bis{2-ethanesulfonic acid}, disodium salt, pH 6.8), resuspended in buffer to ∼10^8 cells mL^{-1} concentration, and made anaerobic by bubbling with O_2-free N_2 gas before being used as inoculum (0.5 mL of cell suspension to 10 mL culture tubes). Culture tubes were incubated on their side, without shaking and in the dark at 31 °C. Standard anaerobic techniques were used for all procedures as described in ref *16*.

* Corresponding author phone: (205)348-5191; fax: (205)348-1403; e-mail: murrutia@biology.as.ua.edu.
† This work is dedicated to the memory of Laureano Urrutia.
‡ The University of Alabama.
§ Pacific Northwest National Laboratory.

10.1021/es990447b CCC: $18.00
Published on Web 09/29/1999

Synthesis of Fe(III) Goethite. Goethite (Gt) was synthesized and treated as explained previously (*3*). The mineral obtained had a surface area of 55 $m^2\ g^{-1}$ as determined by five-point BET N_2 adsorption.

Influence of EDTA and NTA Concentration on Gt Reduction. Chelators were added to culture tubes (30 mM malate, 0.04 mM P, pH 6.8) in triplicate from filter sterilized, anaerobic stock solutions (1, 5, 10, 50, 100, and 500 mM) to obtain final concentrations of 0.01, 0.05, 0.1, 0.5, 1.0, or 5.0 mM. The stocks were prepared with the tetrasodium salt of EDTA (Na_4EDTA) (Fisher Scientific) and the disodium salt of NTA (Na_2HNTA) (Sigma Chem. Co.). Tubes were inoculated with washed TSB-grown *S. alga* cells immediately following chelator addition. Duplicate sterile controls were included for each chelator concentration. Soluble Fe(II) and Fe(III), and HCl-extractable Fe(II), were determined at 1, 3, 7, 15, and 30 day intervals.

Effect of Chelators on Fe(II) Adsorption onto Gt. The influence of the chelators on Fe(II) sorption by Gt was evaluated by addition of soluble Fe^{2+} (added as $FeCl_2$) to 50 mmol L^{-1} suspensions of the mineral in the presence and absence of 0.5 mM EDTA or NTA under strictly anaerobic conditions. The Fe(II) sorption capacity of this mineral (in 10 mM Pipes buffer at pH 6.9 without chelators) had been characterized previously (*3*) as 0.25 mmol Fe(II) g^{-1}. EDTA or NTA (0.1 mL) was added to triplicate 10-mL portions of sterile Gt suspension in Pipes buffer (10 mM, pH 6.9) from filter sterilized anaerobic stocks. Immediately afterward, a 0.2-mL aliquot of an anaerobic, filter-sterilized $FeCl_2$ stock solution was added to each tube to obtain Fe(II) concentrations ranging from 0.032 to 5.12 mM. Samples were allowed to equilibrate for 18 h with gentle shaking (50 rpm on a rotary shaker), after which the concentration of aqueous Fe(II) [$Fe(II)_{aq}$] was determined as described below. The difference between total added Fe(II) and $Fe(II)_{aq}$ was taken to represent sorbed Fe(II).

Adsorption of Fe(II)−Chelator Complexes onto Gt. Equimolar volumes of anaerobic Fe(II) (as $FeCl_2$) and EDTA (as Na_4EDTA) or NTA (as Na_2HNTA) solutions (all prepared in 10 mM Pipes buffer at pH 6.9) were first mixed together in a 1:1 ratio, yielding final Fe(II) and chelator concentrations of 10 mM. After a period of 6 h, different amounts of this Fe(II)−EDTA or Fe(II)−NTA solution were added to 50 mmol L^{-1} suspensions of Gt (in 10 mM pipes buffer, pH 6.9), yielding final Fe(II)−chelator concentrations of 0.01, 0.05, 0.13, 0.33, 0.5, and 1 mM. After an 18-h equilibration period with shaking at 50 rpm, $Fe(II)_{aq}$ and 0.5 M HCl-extractable Fe(II) were analyzed. Adsorbed Fe(II) (as Fe(II)−EDTA or Fe(II)-NTA) was calculated from the difference between $Fe(II)_{aq}$ and total Fe(II) extracted in HCl (see below).

Fe(II) Speciation Calculations. The program MINTEQA2 (*17*) was used to model the adsorption of Fe(II) onto Gt in the presence of chelators (using the equilibrium constants for Fe(II)−chelator complexes formation included in Table 1, Supporting Information), and the adsorption of Fe(II)−chelators onto Gt. MINTEQA2 was also used to model results obtained at the end of the reduction experiments in the presence of NTA or EDTA. The modeling approach adopted here is explained in detail elsewhere (*3*).

Experiments with Solid-Phase Fe(II) Complexants. Two types of experiments were conducted (in 8 mM malate, 0.04 mM P media): some in which goethite, cells and the solid-phase Fe(II) sink (either aluminum oxide or layered silicates) were allowed to be in direct contact, and some in which the Fe(II) sink was separated from the goethite and cells by inclusion in a dialysis bag. The later approach allowed the exchange of solutes but avoided contact of the cells with the clay/Al mineral.

The minerals used were Al_2O_3 (adsorption grade alumina, 80−200 mesh particle size, Fisher Sci., surface area 113 $m^2\ g^{-1}$) and three phyllosilicate minerals, commercial kaolin (Ka) (external surface area 16 $m^2\ g^{-1}$), Aldrich KSF montmorillonite (KSF) (external surface area 7 $m^2\ g^{-1}$), and Aldrich K10 montmorillonite (K10) (external surface area 246 $m^2\ g^{-1}$) (all from Aldrich Chem. Co.). Surface areas were obtained by five-point BET N_2 adsorption in a Micromeritics Gemini 2360 surface area analyzer, after 2 h degassing under N_2 atmosphere at 200 °C in a Micromeritics Flowprep 060. HCl-extractable Fe in the layer silicates was determined with 12 M HCl, yielding values of 0.183 mmol Fe per gram of KSF, 0.064 mmol g^{-1} for K10, and only traces (0.0011 mmol g^{-1}) for Ka. Fe(II) and Fe(III) solubilized from the montmorillonites before and after autoclaving (as may occur in culture experiments) were also determined (Table 2, Supporting Information). The KSF montmorillonite produced significant amounts of HCl-extractable Fe(II) and Fe(III) upon resuspension in aqueous media as well as some aqueous Fe(II) and Fe(III). The K10 montmorillonite, on the other hand, contained practically no Fe(II), but some soluble and HCl-extractable Fe(III) (Table 2, Supporting Information). Because of the Fe content of the montmorillonite clays, total Fe in these reduction experiments was calculated as the sum of Fe(III) in Gt plus Fe(III/II) in the clay mineral (when present).

Direct Contact Experiments. The mineral solids were added to 50 mmol L^{-1} Gt suspensions (248 $m^2\ L^{-1}$) in the following concentrations: 1.0 or 5.0 g L^{-1} of Al_2O_3 (total surface area concentration of 113 or 565 $m^2\ L^{-1}$, respectively), 2.6 or 13.0 g L^{-1} of Ka (42 or 208 $m^2\ L^{-1}$, respectively), 3.7 or 18.5 g L^{-1} of KSF (26 or 130 $m^2\ L^{-1}$, respectively) or K10 (910 or 4551 $m^2\ L^{-1}$, respectively) (equivalent to solid in suspension concentrations of 10 and 50 mmol L^{-1}, respectively). Cultures were set up as explained above. Samples were collected aseptically and anaerobically at 1, 2, 7, 9, 15, 30, and 40 days after inoculation for Fe(II) determination as described below. Fe reduction was compared to controls with Gt only.

Dialysis Bag Experiments. Dialysis bags (Spectra/Por 1.1 Biotech sterile membranes, 8000 MWCO, 5 mL sample volume) were used to prevent bacterial attachment to the solid-phase complexants. In these experiments, 1 g L^{-1} aluminum oxide was sterilized in 1 mL of 10 mM Pipes buffer (pH 6.8) and aseptically transferred into a sterile dialysis bag. The same procedure was used with both concentrations of layer silicates. The bags were then aseptically introduced into anaerobic goethite in culture medium flasks inside an anaerobic chamber. Once resealed, H_2 gas was added, and samples were inoculated with *S. alga* cells as explained above. Fe reduction was compared to controls with the alternative Fe(II) sinks in direct contact with Gt. The aluminum oxide and layer silicates inside the dialysis bags were not sampled for Fe(II) until the last sampling date (30 days). For this analysis, cultures were taken into the anaerobic chamber, and the dialysis bags were collected and digested in 0.5 M HCl (see Analytical Techniques section). The total amount of Fe in the goethite suspensions was also determined at this time. In another repetition of this experiment, triplicate cultures were set up with 1 g L^{-1} aluminum oxide or 2.6 g L^{-1} Ka inside dialysis bags; empty dialysis membranes were introduced in triplicated Gt control cultures as well. Reduction of the Gt by *S. alga* was followed over time, and the Fe(II) content of dialysis membranes and the mineral complexants were analyzed at the completion of the experiment (30 days) as indicated above.

Adhesion Test. Adhesion of *S. alga* cells to goethite and aluminum oxide minerals was studied following the method of Caccavo et al. (*18*), modified for our experimental system. Pipes (10 mM, pH 6.9) was used as adhesion buffer as in all our reduction experiments. Total cell numbers determination was obtained from cell counts in control tubes to which no mineral was added (Pipes only), because neither goethite nor aluminum oxide were dissolved by the methodological

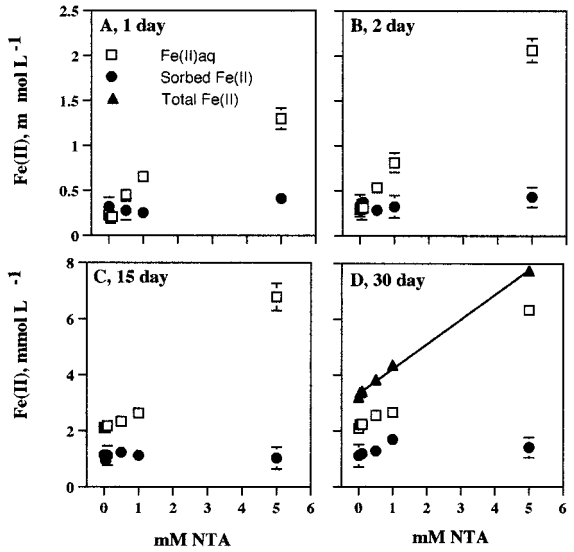

FIGURE 1. Reduction of Gt (50 mmol L^{-1}) by *S. alga* in the presence of different NTA concentrations after 1, 2, 15, and 30 days. Fe(II) was speciated into soluble Fe(II), ($Fe(II)_{aq}$), and sorbed Fe(II); total Fe(II) (soluble + sorbed) is included for the 30 d sample. Data represent the mean ± standard deviation of triplicate cultures; nonvisible error bars are smaller than the corresponding symbol. The solid line in panel D represents a linear regression analysis of total Fe(II) as a function of NTA concentration ($r^2 = 0.997$).

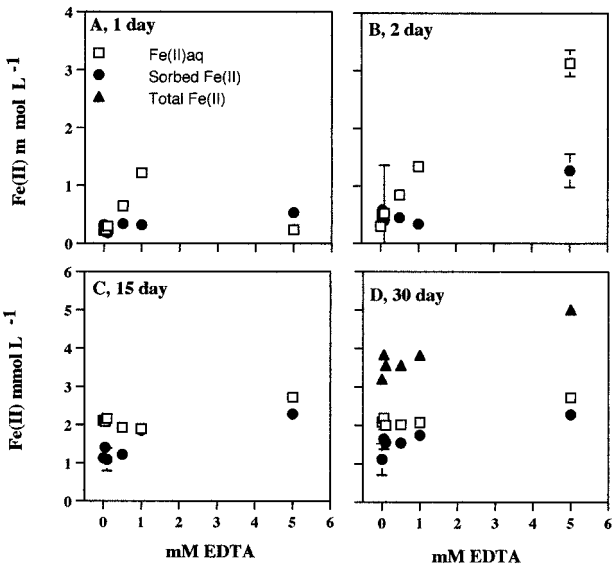

FIGURE 2. Reduction of Gt (50 mmol L^{-1}) by *S. alga* in the presence of several EDTA concentrations at 1, 2, 15, and 30 days. Fe(II) was speciated into soluble ($Fe(II)_{aq}$) and sorbed Fe(II); total Fe(II) (soluble + sorbed) is included for the 30 d sample. Data represent the mean ± standard deviation of triplicate cultures; nonvisible error bars are smaller than the corresponding symbol.

procedure used in Caccavo et al. (*18*). Adhesion of cells to aluminum oxide was compared to adhesion to Gt with triplicate tubes in which both minerals were present at equimolar concentrations (50 mM). A triplicate set of tubes with 50 mM Gt and 1 g L^{-1} aluminum oxide as in our reduction experiments was also included.

Analytical Techniques. Total Fe(II) in 0.2−0.5 mL culture samples was determined by extraction with 5 mL of 0.5 M HCl for 2 h, followed by colorimetric analysis of Fe(II) with ferrozine. $Fe(II)_{aq}$ was measured by filtering a 0.2−1.0 mL aliquot of sample through a 0.22 μm nylon syringe filter directly into ferrozine and reading the A_{562} immediately. Total Fe in aqueous phase samples and HCl extracts was obtained by reducing all Fe(III) with $NH_2OH{\cdot}HCl$ prior to colorimetric Fe determination. Fe(III) concentrations were calculated from the difference between total Fe and Fe(II).

Preliminary experiments showed a very slow color development during the Fe(II) ferrozine colorimetric assay in the presence of EDTA, most likely due to competition between EDTA and ferrozine for Fe(II). Therefore, standard curves were prepared with Fe(II) and Fe(III) standard solutions having EDTA concentrations equal to those used in the reduction experiments. Fe(II) (0.1, 0.2, 0.5, and 1 mM) was added as ferrous diammonium sulfate, and Fe(III) (0.1, 0.2, 0.5 and 1 mM) as $FeCl_3$. EDTA concentrations were 0.05, 0.1, 0.5, 1, and 5 mM for Fe(II) standard curves and 5 mM for Fe(III). Both Fe(II) and Fe(III) standard curves with 5 mM NTA were also prepared to test the effect of NTA on color development; the presence of NTA did not cause any interference with the assay. Regression equations obtained with each EDTA concentration were used to correct sample A_{562} readings in all subsequent experiments. Neither EDTA nor NTA caused any interference in the determination of Fe(III).

Results

Influence of EDTA or NTA on Gt Reduction. The presence of increasing NTA concentrations led to consistent enhancement of the initial (0−48 h) Gt reduction by *S. alga*, due to increases in $Fe(II)_{aq}$ (Figure 1A,B). A small amount of Fe(III) (maximum of 15 μmol Fe(III) L^{-1}) was dissolved from Gt by the highest NTA concentration (5 mM) in sterile controls (data not shown), whereas no $Fe(III)_{aq}$ was ever detectable in NTA-amended *S. alga* cultures. After a week to 1 month of incubation, Fe(III) reduction increased proportionally ($r^2 = 0.997$) to NTA concentration (Figure 1D). The increase in Fe(III) reduction was caused by solubilization of Fe(II) by NTA; there was no substantial effect of NTA on sorbed Fe(II) (closed circles).

The presence of increasing concentrations of EDTA noticeably enhanced initial Gt reduction by *S. alga* in relation to the nonchelator controls (Figure 2A,B). As with NTA, this effect was due to increases in the $Fe(II)_{aq}$ fraction (open squares in figure). The only exception was the samples to which 5 mM EDTA was added (Figure 2A). EDTA solubilized up to 25 μmol Fe(III) L^{-1} from goethite after 2 days and up to 100 μmol Fe(III) L^{-1} after 30 days in the sterile controls amended with 0.5 or 1 mM EDTA. $Fe(III)_{aq}$ was negligible in EDTA-amended *S. alga* cultures. The long-term extent of Gt reduction was not significantly increased by addition of EDTA at concentrations ≤1 mM ($p < 0.01$) (Figure 2D). The cultures that received 5 mM EDTA over time also showed increases in both $Fe(II)_{aq}$ and sorbed Fe(II) (Figure 2B,C). The final extent of goethite reduction was enhanced 25% by 5 mM EDTA in relation to the nonchelator controls (Figure 2D).

Influence of EDTA and NTA on Fe(II) Sorption by Goethite. Fe(II) adsorption isotherms were conducted in the presence of 0.5 mM NTA or EDTA under pH and ionic strength conditions identical to those in the Gt reduction experiments (Figure 3 A,B). The presence of 0.5 mM NTA reduced Fe(II) sorption at low Fe(II) loadings but did not significantly affect the amount of Fe(II) sorbed at near saturation levels (Figure 3A). The presence of 0.5 mM EDTA had a similar effect (Figure 3B). Fe(II) sorption at low Fe(II) loadings was slightly greater in the presence of EDTA than in the presence of NTA. The point on the isotherm below which the chelators influenced Fe(II) sorption is $10^{-3.3}$ mol L^{-1}, which is the added chelator concentration. This result was foreseen, since chelators would be expected to affect Fe(II) sorption only when the total chelator concentration is greater than the total Fe(II) concentration.

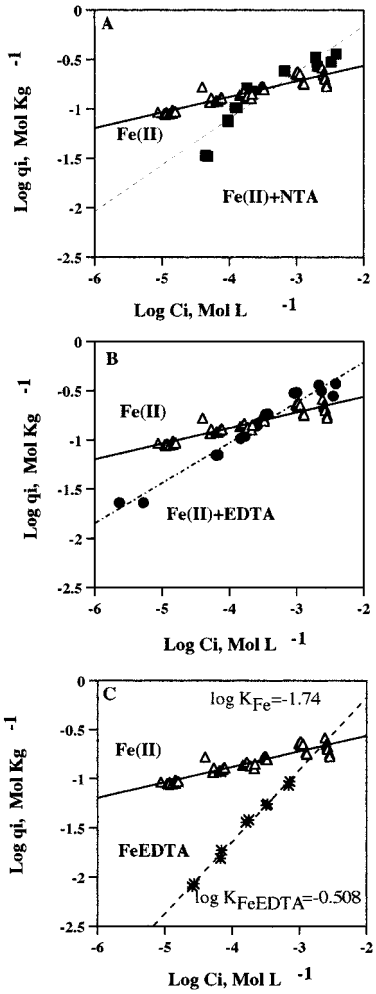

FIGURE 3. Fe(II) adsorption onto goethite (50 mmol L^{-1}) in the presence of NTA or EDTA. (A) Freundlich plot for Fe(II) adsorption onto Gt in the presence of 0.5 mM NTA (Fe(II) + NTA) (solid squares ■). (B) Freundlich plot for Fe(II) adsorption onto Gt in the presence of 0.5 mM EDTA (Fe(II) + EDTA) (solid circles ●). (C) Freundlich plot for adsorption of Fe(II)−EDTA complexes onto Gt (FeEDTA) (stars ∗). A previously determined (*3*) isotherm for uncomplexed Fe(II) adsorption to the same Gt mineral in the absence of chelators is included in each panel as a reference (open triangles △) (reproduced with permission from the publisher, Taylor & Francis, Ltd). Each point represents an individual sample. Ci = soluble Fe(II) at equilibrium; qi = adsorbed Fe(II) at equilibrium; Freundlich equations: Fe(II) adsorption in Pipes buffer, $y = 0.158x - 0.246$, $r^2 = 0.858$; Fe(II) adsorption in the presence of 0.5 mM NTA, $y = 0.469x + 0.777$, $r^2 = 0.860$; Fe(II) adsorption in the presence of 0.5 mM EDTA, $y = 0.409x + 0.609$, $r^2 = 0.965$; FeEDTA adsorption, $y = 0.733x + 1.287$, $r^2 = 0.993$. Log K_F values in (C) are derived from activity Freundlich transforms of the data using MINTEQA2.

Adsorption of Fe(II)−Chelator Complexes onto Goethite. Adsorption of Fe(II)−EDTA to Gt was low at low sorbate concentrations but at high loadings approached the levels of uncomplexed Fe(II) adsorption (Figure 3C). The adsorption data were fit to an activity Freundlich adsorption model using MINTEQA2 ($\log K_F = -0.508$). Fe(II)−NTA complexes sorbed much less strongly than Fe(II)−EDTA (data not shown).

Calculated Fe(II) Speciation. The equilibrium speciation of Fe(II) was computed as a function of chelator concentration (Table 3) to assess the potential solid and aqueous phase associations of biogenic Fe(II). The total Fe(II) concentration chosen for these calculations was 3.2 mmol L^{-1}, equal to the average amount of reduction obtained in the nonchelator controls at the end of the experiment (Figures 1D and 2D). Values for Fe(II)−chelator complexes equilibrium constants are compiled in Table 1, Supporting Information. Although the experimental Fe(II) speciation obtained in Fe reduction experiments is not always accurately described by these computations ((*3*)), they should nevertheless give an idea of the major speciation trends in the presence of the chelators. Fe(II) speciation calculations in the presence of EDTA (0.5−5 mM) were conducted to obtain equilibrium concentrations for all the Fe(II)−EDTA species. The most abundant Fe(II)-EDTA species under these conditions, $FeEDTA^{2-}$, was then considered to be the sorbing species. $FeEDTA^{2-}$ adsorption to Gt was then included with an activity Freundlich model (Figure 3C); for each EDTA concentration, the initial total $FeEDTA^{2-}$ was the equilibrium concentration for this species obtained previously. This approach allowed $FeEDTA^{2-}$ to distribute between $FeEDTA^{2-}_{aq}$ and $FeEDTA^{2-}_{sorbed}$ according to the measured isotherm (Figure 3C). These calculations revealed significant increases in $FeEDTA^{2-}_{sorbed}$ with increasing EDTA concentration that took place at the expense of the aqueous components (Table 3). These results agreed with the Fe(II) speciation observed in Gt reduction experiments in the presence of EDTA (Figure 2), in which there was an increase in the sorbed Fe(II) fraction in relation to nonchelator controls (note that solid-phase Fe(II) determinations do not differentiate what chemical species of Fe(II) is being measured).

Calculations for Fe(II) speciation in the presence of NTA (0.5−5 mM) indicated that $FeNTA^-$ was the predominant Fe(II)−NTA species for NTA concentrations ≤1 mM, whereas both $FeNTA^-$ and $FeNTA_2^{4-}$ were equally abundant at 5 mM NTA levels (Table 3). Increasing concentrations of NTA led to stepwise increases in $Fe(II)NTA_{aq}$ species at the expense of vivianite ($Fe_3(PO_4)_2 \cdot 8H_2O$), Fe(II)−malate complexes, and $Fe(II)_{sorbed}$ (from a total of 0.86 mmol L^{-1} in absence of NTA to 0.13 mmol L^{-1} with 5 mM NTA). Sorption of $FeNTA^-$ species ($FeNTA^-_{sorbed}$) was computed to be very low based on experimental data (Table 3). Consolidated budgets for $Fe(II)_{aq}$ and solid-phase Fe(II) for this exercise showed that $Fe(II)_{aq}$ would increase with increasing NTA concentrations through solubilization of the solid-phase Fe(II) fraction (Table 3). These results were conceptually consistent with experimental observation (Figure 1).

Solid-Phase Fe(II) Sinks. The reduction of goethite by *S. alga* was suppressed when Al_2O_3 particles were in direct contact with Gt and cells (Figure 4 A,B, filled diamonds). Cell adhesion assays showed that the cells adhered much strongly to Gt than to aluminum oxide, but there was measurable cell adhesion to the Al mineral. Overall a 70−75% cells were adhered in tubes with Gt (with or without aluminum oxide) versus around 20% in tubes with aluminum oxide only. When the aluminum oxide was enclosed inside a dialysis bag, which allowed exchange/diffusion of solutes but avoided contact between cells and the Al_2O_3, Gt was reduced more readily than in the absence of the Al mineral (Figure 4, open circles). At the end of the experiment, the alumina inside the dialysis bag had bound up to 12 mmol Fe L^{-1}, which represents 25% of the Fe(III) present initially in the goethite. Overall, the total amount of Fe(III) reduced in this system was approximately 35% of the total, in comparison to 7−10% reduced in absence of the aluminum oxide. A subsequent experiment (Figure 5) confirmed that Gt reduction was promoted by the presence of aluminum oxide due to sorption/binding of Fe(II) onto the Al mineral and the dialysis bag (Figure 5), since some Fe(II) was also bound by the dialysis bag itself.

Kaolinite in direct contact with the cells/goethite decreased Gt reduction (data not shown). When Ka was placed in a dialysis membrane, approximately 15% of the initial Fe(III) content was bound as Fe(II) by Ka at the end of the

TABLE 3. Calculated Fe(II) Speciation (MINTEQA2) in Presence of Different Concentrations of NTA or EDTA[b]

species	0 mM	0.1 mM	0.5 mM	1 mM	5 mM
			NTA		
Fe^{2+}	2.1×10^{-4}	2.0×10^{-4}	1.7×10^{-4}	1.4×10^{-4}	8.1×10^{-6}
$FeHPO_{4aq}$	1.3×10^{-7}	1.3×10^{-7}	1.4×10^{-7}	1.6×10^{-7}	7.2×10^{-8}
FeMalate	2.1×10^{-3}	2.0×10^{-3}	1.7×10^{-3}	1.4×10^{-3}	7.8×10^{-5}
$FeNTA^{1-}{}_{aq}$	0	9.8×10^{-5}	4.8×10^{-4}	9.2×10^{-4}	1.4×10^{-3}
$FeNTA_2^{4-}$	0	2.4×10^{-7}	6.8×10^{-6}	3.2×10^{-5}	1.6×10^{-3}
FeHNTA	0	1.3×10^{-9}	6.4×10^{-9}	1.2×10^{-8}	1.9×10^{-8}
$FeOHNTA^{2-}$	0	1.6×10^{-8}	7.9×10^{-8}	1.5×10^{-7}	2.4×10^{-7}
Fe_{sorbed}[a]	8.6×10^{-4}	8.4×10^{-4}	7.7×10^{-4}	6.8×10^{-4}	1.3×10^{-4}
Vivianite[a]	5.6×10^{-5}	5.5×10^{-5}	5.4×10^{-5}	5.2×10^{-5}	0
$FeNTA^{1-}{}_{sorbed}$[a]	0	4.1×10^{-7}	7.3×10^{-7}	9.3×10^{-7}	1.4×10^{-7}
Fe(II)aq total	2.3×10^{-3}	2.3×10^{-3}	2.4×10^{-3}	2.5×10^{-3}	3.1×10^{-3}
Solid-phase total	9.2×10^{-4}	9.0×10^{-4}	8.2×10^{-4}	7.3×10^{-4}	1.3×10^{-4}
			EDTA		
Fe^{2+}	2.1×10^{-4}	2.0×10^{-4}	1.7×10^{-4}	1.4×10^{-4}	3.5×10^{-11}
$FeHPO_{4aq}$	1.3×10^{-7}	1.3×10^{-7}	1.4×10^{-7}	1.6×10^{-7}	3.1×10^{-13}
FeMalate	2.1×10^{-3}	2.0×10^{-3}	1.7×10^{-3}	1.3×10^{-3}	3.4×10^{-10}
$FeEDTA^{2-}{}_{aq}$	0	3.0×10^{-5}	2.1×10^{-4}	4.7×10^{-4}	1.8×10^{-3}
$FeHEDTA^{-}$	0	7.6×10^{-9}	3.8×10^{-8}	7.6×10^{-8}	2.4×10^{-7}
$FeOHEDTA^{3-}$	0	5.8×10^{-7}	2.9×10^{-6}	5.8×10^{-6}	1.9×10^{-5}
$Fe(OH)_2EDTA^{4-}$	0	3.6×10^{-9}	1.8×10^{-8}	3.7×10^{-8}	1.3×10^{-7}
Fe_{sorbed}[a]	8.6×10^{-4}	8.4×10^{-4}	7.7×10^{-4}	6.7×10^{-4}	1.3×10^{-7}
Vivianite[a]	5.6×10^{-5}	5.6×10^{-5}	5.4×10^{-5}	5.2×10^{-5}	0
$FeEDTA^{-2a}{}_{sorbed}$	0	6.9×10^{-5}	2.9×10^{-4}	5.2×10^{-4}	1.4×10^{-3}
Fe(II)aq total	2.3×10^{-3}	2.2×10^{-3}	2.1×10^{-3}	1.9×10^{-3}	1.8×10^{-3}
Solid-phase total	9.1×10^{-4}	9.6×10^{-4}	1.1×10^{-3}	1.2×10^{-3}	1.4×10^{-3}

[a] Solid-phase Fe(II). [b] The total Fe(II) concentration in the modeled system (3.2×10^{-3} M) was equal to the amount generated during reduction experiments in the nonchelator cultures (see text). Only major species are presented. Concentrations are in units of mol L^{-1}.

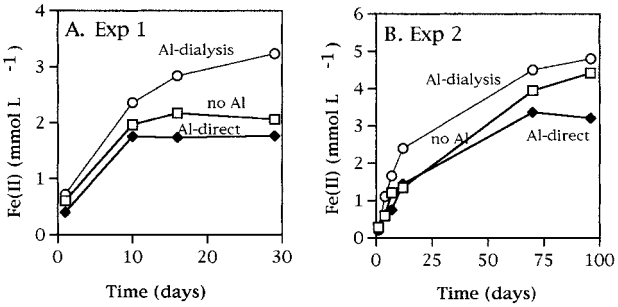

FIGURE 4. Reduction of Gt (50 mmol L^{-1}) by *S. alga* in the presence of Al_2O_3 (1 g L^{-1}) inside a dialysis bag (open circles) or in direct contact with the cells (filled diamonds) in comparison to a non-Al_2O_3 control (no Al, open squares). (A) Initial experiment. (B) Second experiment. Fe(II) concentrations reflect the Fe(II) content of the Gt suspension only (dialysis bag was not analyzed until the final sampling date). Data represent the mean ± standard deviation of triplicate cultures; nonvisible error bars are smaller than the corresponding symbol.

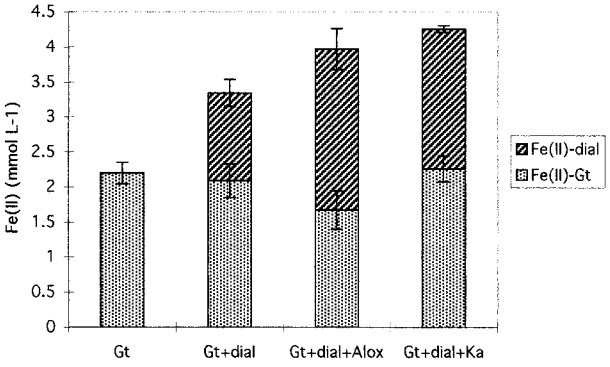

FIGURE 5. Reduction of Gt (50 mmol L^{-1}) by *S. alga* with or without Al_2O_3 (1 g L^{-1}) or kaolinite (2.6 g L^{-1}) within dialysis bags after 30 d incubation. Control cultures containing an empty dialysis bag were included. Fe-Dial: HCl-extractable Fe(II) contained in the dialysis bag and the enclosed solid. Fe-Gt: HCl-extractable Fe(II) from goethite at the end of the experiment. Data represent mean ± standard deviation of triplicate cultures.

experiment (Figures 5 and 6), enhancing Gt reduction by 2-fold.

The presence of K10 or KSF montmorillonites in direct contact with the cells either had no effect or slightly hindered Gt reduction (data not shown). When the montmorillonites were enclosed inside the dialysis bag, the total amounts of Fe(II) determined in the Gt suspension (outside the dialysis bag) were lower than in direct contact experiments. However, the K10 and KSF inside the dialysis bag bound significant quantities of Fe(II) at experiment termination, which led to a dramatic increase in total Fe(II) production (Figure 6).

Discussion

Effect of Synthetic Chelators. Previous studies suggested that NTA stimulated iron(III) oxide reduction in aquifer sediments due to solubilization of Fe(III), since laboratory tests (with ~2−4 mM NTA) demonstrated this chelator's ability to solubilize Fe(III) from amorphous iron oxides (*12*). Our results suggest that chelators can stimulate crystalline iron(III) oxide (goethite) reduction by this same mechanism, although the magnitude of the effect is much reduced due to the lower solubility of goethite. This solubilization effect was demonstrated by the enhanced initial rates of reduction with increasing chelator concentrations (Figures 1 and 2). The solubilization effect was more significant with EDTA (Figure 2) than NTA (Figure 1), because EDTA is a stronger Fe(III) ligand (log $K_{Fe(III)NTA}$= 17.83, log $K_{Fe(III)EDTA}$ = 27.57, (*19*)). EDTA solubilized more Fe(III) in sterile controls, with maximum values of 100 μmol L^{-1} after 1 week for 0.5 and 1 mM EDTA concentrations. Similar levels of goethite dissolution (between 40 and 60 μM Fe(III)) by >1 mM EDTA were reported by Davis and Upadhyaya (*20*).

Our results demonstrate that an even greater impact of chelators on iron(III) oxide reduction results from aqueous Fe(II) complexation. Formation of soluble Fe(II) complexes

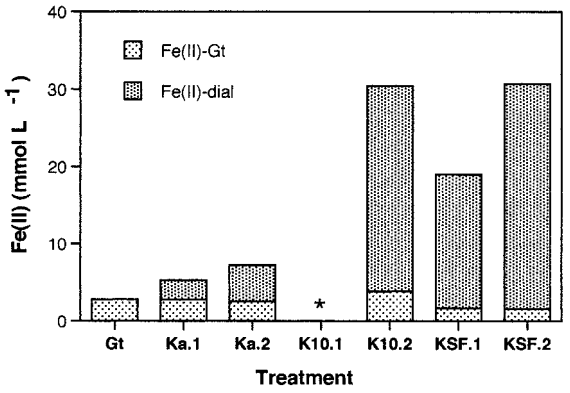

FIGURE 6. Reduction of Gt (50 mmol L^{-1}) by *S. alga* in the presence of layer silicates placed inside dialysis bags after a 30 d incubation. Data for montmorillonites (K10 and KSF) was corrected for (1) soluble Fe(III) released from the clays to the growth medium after autoclaving (see Table 2) and (2) HCl-extractable Fe(II) content of clays.* culture lost. Nomenclature: Ka.1 = 2.6 g clay L^{-1}; Ka.2 = 13 g clay L^{-1}; K10.1 = 3.7 g clay L^{-1}; K10.2 = 18.5 g clay L^{-1}; KSF.1 = 3.7 g clay L^{-1}; KSF.2 = 18.5 g clay L^{-1}.

in NTA amended cultures led to increases in $Fe(II)_{aq}$ concentration in direct proportion to the chelator concentration (Figure 1). These increases in $Fe(II)_{aq}$ were associated with a parallel increase in total Fe(III) reduction. In similar manner, complexation of evolved Fe(II) during iron(III) oxide reduction promoted reduction of goethite in the presence of the much weaker (compare log $K_{Fe(II)malate} = 3.48$ with values in Table 1, Supporting Information) organic chelator malate (*3*). Speciation calculations indicated that aqueous Fe(II)−NTA species formed mainly at the expense of the solid-phase Fe(II) pool (Table 3), particularly at NTA concentrations greater than 1 mM, and that sorption of Fe(II)−NTA species to Gt was insignificant. These calculations suggest that NTA enhanced bacterial reduction of goethite through formation of soluble Fe(II) complexes. The decrease in Fe(II) adsorption to Gt (Figure 3A) when NTA was in greater than equimolar concentration further support this conclusion.

In the case of EDTA, we observed that Fe(II)−EDTA complexes adsorbed to goethite (Figure 3C). Several metal−EDTA complexes are known to sorb to iron(III) oxides with increasing affinity at lower pH (*21*−*23*), including both Fe(III)−EDTA (*7*, *8*, *24*, *25*) and Fe(II)−EDTA (*13*). These later authors observed that $Fe(II)EDTA^{2-}$ complexes, which formed through dissociation of $Co(II)EDTA^{2-}$ in their system, exhibited comparable sorptivity to both the starting and bioreduced goethite mineral.

Sorption of $Fe(II)EDTA^{2-}$ may partly account for the increases in sorbed Fe(II) observed in samples amended with 5 mM EDTA (Figure 2D). Such sorption may also be reponsible for the smaller effect of EDTA, compared to NTA, on Gt reduction despite the higher stability of the Fe(II)-$EDTA^{2-}$ complex (log $K = 15.98$ for $Fe(II)EDTA^{2-}$ vs log $K = 9.85$ for $Fe(II)NTA^{-}$, Table 1, Supporting Information). The Fe(II) speciation calculations that included adsorption of $FeEDTA^{2-}$ to Gt (Table 3), which showed that there was no predicted increase in $Fe(II)_{aq}$ with increasing EDTA concentrations, support this conclusion.

Effect of Complexing Solids. Our initial experiments showed that aluminum oxide in direct contact with FeRB inhibited Gt reduction. Tests indicated that cells adhered to aluminum oxide, although to a lesser extent than to Gt (∼20% adhesion to Al_2O_3 vs 70−75% adhesion to Gt). A 20% reduction of the initial cell concentration added at inoculation (∼5 × 10^8 cells mL^{-1}) would leave an active population of approximately 4 × 10^8 cells mL^{-1}. Previous observations found significant decreases in Fe(III) reduction rates (of both HFO and Gt) with decreasing cell densities, particularly for cell densities lower than 6 × 10^8 cells mL^{-1} (*4*). Hence it is reasonable to expect an apparent decrease in Gt reduction in direct contact experiments due to adhesion of cells onto the accompanying aluminum oxide.

The argument and data above were further corroborated by the enhancement of Gt reduction observed when the aluminum oxide was enclosed in a dialysis bag that prevented adhesion of the cells to the aluminum oxide (Figures 4 and 5). In this case, approximately equal quantities of Fe(II) were found in the Gt suspension and aluminum oxide at completion of the experiment (Figure 5), overall doubling the total amount of Gt reduced in relation to the non-aluminum oxide control. Fe(II) sorption capacities for these minerals (normalized to surface area) are 6.4 μmol Fe(II) m^{-2} for the Gt and 4.4 μmol Fe(II) m^{-2} for the Al_2O_3. After 30 days incubation, around 25% of the total HCl-extractable Fe(II) in the growth medium (8 mM malate, 0.04 mM P) is present as $Fe(II)_{aq}$. Therefore, for the data presented in Figure 5, Gt was approximately 75% saturated with Fe(II) (5.05 μmol Fe(II) m^{-2}), and the aluminum oxide had about 1.5 times more Fe(II) (6.9 μmol Fe(II) m^{-2}) than the measured saturation level (4.4 μmol Fe(II) m^{-2}). These results suggest that the Fe(II) sorption by the aluminum oxide mineral and, possibly, surface precipitation mechanisms serve to partition Fe(II) away from active reduction surfaces on Gt and FeRB cells, thereby promoting the extent of Gt reduction.

The presence of the silicates in direct contact with cells and Gt generally did not enhance Fe(II) production (data not shown). Layer silicates and iron(III) oxides (*27*) or bacterial walls (*28*) have been shown to form aggregates when in contact. Therefore, blockage of surface sites involved in Fe(III) reduction via aggregation may have been responsible for the observed results. When this physical impediment was removed (dialysis bag experiments), the presence of kaolinite (Ka) (Figures 5 and 6) or montmorillonite (K10 and KSF) (Figure 6) greatly promoted the long-term extent of Gt reduction by *S. alga*.

Our results demonstrate that, under appropriate conditions, aluminum oxides and layer silicates enhance bacterial iron(III) oxide reduction by drawing biogenic Fe(II) away from the iron(III) oxide and cell surfaces. The solid-phase complexants compete for Fe(II) and delay surface passivation of the iron(III) oxide and cells. The inhibition of reduction which occurred in the direct contact experiments is not meaningful for natural environments, because established in situ populations of FeRBs would preferentially colonize the surfaces of the iron(III) oxides. In soils and sediments, layer silicates and aluminum/iron oxides are commonly found as discrete phases and, as such, could perpetuate the reduction of iron(III) oxides by the mechanisms mentioned above.

In conclusion, the long term extent of iron(III) oxide reduction may be enhanced by aqueous or solid-phase complexants which prevent Fe(II) sorption to the iron oxide and to the bacterial cells. NTA, aluminum oxide, and layer silicate minerals all enhance bacterial iron(III) oxide reduction. In the case of solid-phase Fe(II) complexants, however, physical effects such as adsorption of the cells to non-iron(III) oxide surfaces and/or aggregate formation hindered the positive effect on Fe(III) reduction. EDTA enhanced the long-term extent of reduction only at very high concentrations, probably as a result of $Fe(II)EDTA^{2-}$ complexes sorption to the iron(III) oxide surface. It is feasible that in an open system in which reaction products are eliminated, EDTA may also enhance the total extent of reduction by a continued solubilization of Fe(III). However, under nonflow conditions, concentrations of EDTA lower than 1 mM will not have a substantial effect on the amount of Fe reduced from crystalline iron(III) oxides by FeRB. In the case of NTA, our

results suggest that even low levels of chelator in an advective flow field could substantially enhance the degree of oxide reduction by complexing evolved Fe(II). Other Fe(II) ligands (natural humic or organic acids) could play a similar role. Collectively these findings emphasize the need for including the fate of biogenic Fe(II) in mechanistic models of the rate/extent of iron(III) oxide reduction in sedimentary environments.

Acknowledgments

We would like to thank Ginger Scott for conducting the laborious cell counts. This research was supported by the Subsurface Science Program, Office of Health and Environmental Research, U.S. Department of Energy (DOE), and by the DOE-EMSP Program through Grant No. DE-FG07-96ER62321. Pacific Northwest National Laboratory is operated for DOE by Battelle Memorial Institute under contract DE-AC06-76RLO 1830.

Supporting Information Available

Tables of equilibrium constants for formation of Fe(II)−chelator complexes used in equilibrium speciation calculations, and HCl-extractable and soluble Fe(II) and Fe(III) from the KSF and K10 montmorillonites before and after autoclaving suspensions in growth medium. This material is available free of charge via the Internet at http://pubs.acs.org.

Literature Cited

(1) Lovley, D. R. *Microbiol. Rev.* **1991**, *55*, 259−287.
(2) Lovley, D. R. *J Ind Microbiol* **1995**, *14*, 85−93.
(3) Urrutia, M. M.; Roden, E. E.; Fredrickson, J. K.; Zachara, J. M. *Geomicrobiol. J.* **1998**, *15*, 269−291.
(4) Roden, E. E.; Zachara, J. M. *Environ. Sci. Technol.* **1996**, *30*, 1618−1628.
(5) Girvin, D. C.; Gassman, P. L.; Bolton, J. H. *Soil Sci. Soc. Am. J.* **1993**, *57*, 47−57.
(6) Jardine, P. M.; Taylor, D. L. *Geoderma* **1995**, *67*, 125−140.
(7) Szecsody, J. E.; Zachara, J. M.; Bruckhart, P. L. *Environ. Sci. Technol.* **1994**, *28*, 1706−1716.
(8) Zachara, J. M.; Smith, S. C.; Kuzel, L. S. *Geochim. Cosmochim. Acta* **1995**, *59*, 4825−4844.
(9) Xue, H.; Sigg, L.; Kari, F. G. *Environ. Sci. Technol.* **1995**, *29*, 59−68.
(10) Bolton, H., Jr.; Li, S. W.; Workman, D. J.; Girvin, D. C. *J. Environ. Qual.* **1993**, *22*, 125−132.
(11) Gonsior, S. J.; Sorci, J. J.; Zoellner, M. J.; Landenberger, B. D. *J. Environ. Qual.* **1997**, *26*, 957−966.
(12) Lovley, D. R.; Woodward, J. C. *Chem. Geol.* **1996**, *132*, 19−24.
(13) Zachara, J. M.; Smith, S. C.; Fredrickson, J. K. *Geochim. Cosmochim. Acta* Submitted for publication.
(14) Rosselló-Mora, R. A.; Caccavo, F., Jr.; Osterlehner, K.; Springer, N.; Spring, S.; Schuler, D.; Ludwig, W.; Amann, R.; Vanncanneyt, M.; Schleifer, K. H. *System. Appl. Microbiol.* **1994**, *17*, 569−573.
(15) Lovley, D. R.; Phillips, E. J. P. *Appl. Environ. Microbiol.* **1988**, *54*, 1472−1480.
(16) Lovley, D. R.; Phillips, E. J. P. *Appl. Environ. Microbiol* **1987**, *53*, 1536−1540.
(17) Allison, J. D.; Brown, D. S.; Novo-Gradac, K. J. U.S. Environmental Protection Agency, Athens, GA, 1991.
(18) Caccavo, F. J.; Schamberger, P. C.; Keiding, K.; Nielsen, P. H. *Appl. Environ. Microbiol.* **1997**, *63*, 3837−3843.
(19) Smith, R. A.; Martell, A. E. *NIST Standard reference database 46;* U.S. Department Commerce: Gaithersburg, MD, 1997.
(20) Davis, A. P.; Upadhyaya, M. *Water Res.* **1996**, *30*, 1894−1904.
(21) Zachara, J. M.; Gassman, P. L.; Smith, S. C.; Taylor, D. *Geochim. Cosmochim. Acta* **1995**, *59*, 4449−4463.
(22) Bowers, A. R.; Huang, C. P. *J. Colloid Interface Sci.* **1986**, *110*, 575−590.
(23) Rueda, E. H.; Grassi, R. L.; Blesa, M. A. *J. Colloid Interface Sci.* **1985**, *106*, 243−246.
(24) Nowack, B.; Sigg, L. *J. Colloid Interface Sci.* **1996**, *177*, 106−121.
(25) Nowack, B.; Lutzenkirchen, J.; Behra, P.; Sigg, L. *Environ. Sci. Technol.* **1996**, *30*, 2397−2405.
(26) Grantham, M. C.; Dove, P. M.; DiChristina, T. J. *Geochim. Cosmochim. Acta* **1997**, *61*, 4467−4477.
(27) Swartz, C. H.; Ulery, A. L.; Gschwend, P. M. *Geochim. Cosmochim. Acta* **1997**, *61*, 707−718.
(28) Walker, S. G.; Flemming, C. A.; Ferris, F. G.; Beveridge, T. J.; Bailey, G. W. *Appl. Environ. Microbiol.* **1989**, *55*, 2976−2984.

Received for review April 21, 1999. Revised manuscript received August 24, 1999. Accepted August 30, 1999.

ES990447B

Table 1. Equilibrium constants for formation of Fe(II)-chelator complexes used in equilibrium speciation calculations (I= 0; 25 °C) (Smith and Martell, 1997).

Species	Log K_a
$FeEDTA^{-2}$	15.98
$FeHEDTA^{-}$	19.11
$FeOHEDTA^{-3}$	6.27
$Fe(OH)_2EDTA^{-4}$	13.64
$FeNTA^{-}$	9.85
FeHNTA	12.00
$FeNTA_2^{-4}$	15.34
$FeOHNTA^{-2}$	-1.18

Supporting Information

Table 2. HCl-extractable and soluble Fe(II) and Fe(III) (μmol g^{-1}) from the KSF and K10 montmorillonites before and after autoclaving 3.7 (KSF.1, K10.1) or 18.5 g L^{-1} (KSF.2, K10.2) suspensions in growth medium (0.04 mM PO_4^{3-}, 8 mM malate, 10 mM Pipes buffer, pH 6.9).

Clay	Fe(II)-HCl	Fe(III)-HCl	FeT-HCl	$Fe(II)_{aq}$	$Fe(III)_{aq}$	FeT_{aq}
Before autoclaving						
KSF.1	11.65	115.38	127.03	0.00	74.79	74.79
KSF.2	7.59	97.29	104.88	0.42	54.52	54.84
K10.1	7.66	33.78	41.45	0.00	8.08	8.08
K10.2	3.01	27.37	30.37	0.00	4.42	4.42
After autoclaving						
KSF.1	19.19	63.13	82.31	4.88	48.47	53.35
KSF.2	16.97	62.49	79.46	5.10	43.11	48.21
K10.1	4.48	22.50	26.98	0.00	4.61	4.61
K10.2	3.29	23.52	26.81	0.00	1.20	1.20

Supporting Information